J. Phys. Chem. A **1999,** *103,* 9355−9358

A Density Functional Theory Study of the Gas-Phase Hydrolysis of Dinitrogen Pentoxide

James A. Snyder, Denise Hanway, Julio Mendez, Alan J. Jamka, and Fu-Ming Tao*

Department of Chemistry and Biochemistry, California State University, Fullerton, Fullerton, California 92834

Received: July 22, 1999; In Final Form: September 24, 1999

The gas-phase hydrolysis of N_2O_5 in the clusters of one to four water molecules is investigated by density functional theory calculations. The excess water molecules beyond stoichiometry of the reaction function as a polar solvent medium that stabilizes an ionic pair in the transition state. The reaction energy barrier is progressively diminished by the successive addition of water molecules and is completely eliminated in the cluster of four water molecules, permitting the hydrolysis reaction to proceed directly to products. Atmospheric implications are discussed to understand the reaction mechanisms for the hydrolysis of N_2O_5 in the gas-phase homogeneous conditions as well as in the heterogeneous conditions.

Introduction

The hydrolysis of dinitrogen pentoxide (N_2O_5) produces nitric acid (HNO_3) according to the reaction $N_2O_5 + H_2O \rightarrow 2HNO_3$, while N_2O_5 is produced via the equilibrium reaction $NO_2 + NO_3 \rightleftarrows N_2O_5$. It represents an environmentally important reaction step for the removal of nitrogen originating from atmospheric nitrogen oxides (NO_x). The yield for this reaction peaks following nightfall when atmospheric levels of NO_x are highest. Using a mathematical model for the Los Angeles Basin, Russel et al.[1] concluded that 56% of HNO_3 formed over a 24 h period was generated during the nighttime. Moreover, 41% of this yield resulted from hydrolysis of N_2O_5.

Considerable attention has been given to the surface-catalyzed hydrolysis of N_2O_5.[2−5] However, the hydrolysis of N_2O_5 is not restricted to a heterogeneous reaction mechanism.[6−8] This point is particularly relevant when the gas-phase hydrolysis of N_2O_5 is considered. In bulk aqueous solvent, the hydrolysis reaction proceeds instantaneously to give products. This represents one extreme, the other being the gas-phase hydrolysis for which N_2O_5 is surrounded by only a small number of water molecules. It has proven difficult to obtain accurate measurements of the rate constant for gas-phase hydrolysis of N_2O_5, due to inadequacies with gas chamber models.[6,7,9,10] Therefore, important questions arise relating to the mechanism of the gas-phase hydrolysis reaction and the particular role(s) assumed by the reacting water molecule(s).

For the gas-phase reaction, a crucial question concerns the effect of progressively increasing the number of water molecules in the reaction system. Since the reaction proceeds directly to products in a bulk aqueous environment, it is of interest to know how the increasing number of water molecules affects the energetics of the reaction, particularly the energy barrier from the reactant adduct to the transition state. One expects that the energy barrier will diminish and eventually disappear after a given number of water molecules are introduced into the reaction system.

In a previous study by our group,[11] we performed density functional theory and ab initio calculations on two N_2O_5 hydrolysis reactions. The first reaction mechanism involves a single-step bimolecular reaction between one molecule of N_2O_5 and H_2O:

$$N_2O_5 + H_2O \rightarrow 2HNO_3 \qquad (1)$$

In the second reaction, one molecule of N_2O_5 reacts with two H_2O molecules:

$$N_2O_5 + H_2O + M \rightarrow 2\,HNO_3 + M \qquad (M = H_2O) \quad (2)$$

In this reaction, one water molecule reacts with N_2O_5, while the other functions as a polar-solvent medium (M), which stabilizes an intermediate ion pair resulting from a nucleophilic attack by the first water molecule.[11] We determined that the second reaction is energetically favorable to reaction 1, the activation energy being about 50% lower.[11]

In the present study, we attempt to examine two additional reactions, i.e.

$$N_2O_5 + 3H_2O \rightarrow 2\,HNO_3 + 2H_2O \qquad (3)$$

$$N_2O_5 + 4H_2O \rightarrow 2\,HNO_3 + 3H_2O \qquad (4)$$

It is found that reaction 3 is energetically favorable over both reactions 1 and 2. In reaction 3, two water molecules that are hydrogen-bonded as a H_2O dimer actively participate in the reaction mechanism, while the third water functions as a solvent medium. Although reaction 3 proceeds through a transition state, reaction 4 appears to proceed directly to products, involving no reaction energy barrier.

The results presented here establish a trend among the relative energies associated with the four reactions related to the number of water molecules in the reacting system. It appears that increasing the number of water molecules in the reacting system drastically lowers the energy barrier between the reactant complex and the transition state. The results for reaction 4 imply that the increase in the number of water molecules eventually causes the hydrolysis reaction to proceed without the appearance of a transition state.

Theory and Method

The first step in the hydrolysis of N_2O_5 in reactions 1−3 involves the formation of a stable intermediate complex of the reactants. This is followed by a nucleophilic attack by the oxygen of H_2O on the electrophilic nitrogen atom in N_2O_5. This gives rise to a transition state (TS) complex, which produces a

10.1021/jp992526f CCC: \$18.00

peak on the minimum energy curve of the potential energy surface. The transition state evolves into an intermediate complex of product molecules, which subsequently dissociates to give the final products. For reaction 3, these states are characterized by the following sequence of steps and complexes: $N_2O_5 + 3H_2O \rightarrow N_2O_5(H_2O)_3$ (intermediate-reactant complex) → TS3 (transition state) → $(HNO_3)_2(H_2O)_2$ (nitric acid dimer−water complex) → $2HNO_3 + 2H_2O$ (nitric acid product and water). Similar sequences can be described for reactions 1 and 2.[11]

The energies and equilibrium geometries for the intermediate-reactant complex, transition state, and product complexes have been calculated using density functional theory. The calculations were performed at the B3LYP level, which denotes Becke's three-parameter functional[12−14] with the nonlocal correlation provided by Lee, Yang, and Parr.[15] We have used the split valence basis set 6-31+G(d). In our earlier study,[11] which examined reactions 1 and 2, results were obtained using both the 6-31+G(d) and the larger 6-311++G(d,p) basis set, and it was determined that the two basis sets gave converged results with respect to basis set size for the energies and geometries. Moreover, the early study[11] established that the B3LYP and MP2 methods gave essentially the same results for the transition state geometries and energy changes along the reaction paths for reactions 1 and 2. The calculated geometries of N_2O_5, H_2O, and HNO_3 were also in good agreement with experimental geometries.[11] As a result, the B3LYP method and the 6-31+G(d) basis set should provide reliable results for our present study. Optimization of the transition state geometry was performed using the synchronous transition-guided quasi-Newton (STQN) method[16] and verified by intrinsic reaction coordinate (IRC) calculations.[16,17] Zero-point energy (ZPE) corrections were calculated using computed harmonic frequencies. All calculations were performed using the GAUSSIAN 94 program[18] executed on Digital UNIX and IBM AIX workstations.

Results and Discussion

Table 1 presents values for the total energy (E), ZPE, and zero-point corrected energy (E + ZPE) at the equilibrium geometries for each of the steps in the reaction pathway of reactions 1−3. Figure 1 illustrates the energy level profile for the reaction pathway in reactions 1−4. The energy values correspond to equilibrium geometries, and the values in parentheses are the ZPE-corrected values.

Comparison of the structures for the intermediate-reactant complex and transition state provide useful information on the mechanism. Figure 2 gives the equilibrium geometries for the intermediate reactant complex, transition state, and intermediate product complex for reaction 3. In the reactant complex, the three H_2O molecules are separated into two groups on two opposite sides of the N_2O_5 molecule, one side with two H_2O molecules that form a H_2O dimer and the other with a single H_2O molecule. The oxygen atom of one H_2O molecule in the H_2O dimer approaches a nitrogen atom of N_2O_5, while a hydrogen atom of the second H_2O in the dimer becomes poised for extraction by the central oxygen atom of N_2O_5. The N2−O1 bond length increases from 1.74 to 2.44 Å, while the O8−N2 distance decreases from 2.78 to 1.97 Å. Moreover, the O6−H12 distance decreases from 2.05 to 1.70 Å, and the O11−H9 distance decreases from 1.85 to 1.55 Å. Hence, N_2O_5 begins to dissociate into the NO_3^- and NO_2^+ species, which are paired with H and OH fragments originating from the H_2O dimer.

Table 2 shows the relative energy and selected bond distances changing along the intrinsic reaction coordinate of the pathway for reaction 3. It is interesting that the active OH bonds of the transition state, O8−H9 and O11−H12, remain close to 1.00 Å and are comparable to typical OH distances in hydrogen bond complexes while the N2−O1 bond is almost totally broken. This shows that the breakage of multiple bonds in such a reaction is sequential, instead of being concerted and simultaneous, as one might expect. The system with the active OH bonds going beyond 1.00 Å produces significant charge separations within the H_2O units and is therefore favorably stabilized by the NO_3^- and NO_2^+ species formed, making the overall energy of the system lower than the energy of the transition state.

For the intermediate-reactant complex, the sum of the Mülliken charges over atoms N2, O4, and O5 is 0.44, and over atoms N3, O1, O6, and O7 is −0.35, which become +0.61 and −0.88, respectively, in the transition state. Hence, Mülliken population analysis provides some qualitative verification for the proposed mechanism.

The active involvement of both H_2O molecules in the dimer can be contrasted with the mechanism for reactions 1 and 2, where it was found that only one H_2O molecule actively participates in the reaction.[11] The role of the second water molecule in reaction 2 is likely that of a polar solvent medium, which provides stabilization of the charged pair species in the transition state. In reaction 3 both water molecules in the dimer actively participate in the reaction while the third water acts as a solvent medium to stabilize the charged pair species. A reaction involving an S_N2 mechanism should be favorable in a polar solvent medium. Therefore, although both of the H_2O molecules of the dimer react in reaction 3, they also provide a solvent medium acting to stabilize the charged intermmediate ion-pair.

We have previously shown[11] that the involvement of a second water molecule in reaction 2 lowers the activation energy relative to reaction 1 in which only one water molecule reacts. It is clear from Table 1 and Figure 1 that the presence of a third H_2O molecule provides an additional decrease in the activation energy relative to reactions 1 and 2. The transition state energies for reactions 1−3 are +20.51, +6.43, and −7.04 kcal/mol, respectively, relative to the separate reactant molecules. The corresponding ZPE-corrected values are 21.57, 11.18, and 0.00 kcal/mol. Each addition of one water molecule to the reaction system lowers the relative energy between the reactants and the transition state by approximately 14 kcal/mol (before ZPE correction). This shows that the energy barrier gradually diminishes on the path from reactants to products with the progressive addition of water molecules in the system.

The energies for the intermediate-reactant complexes are −3.79, −13.03, and −17.02 kcal/mol for reactions 1−3, respectively. The difference between these energies and the respective transition state energies gives the energy barrier between the intermediate-reactant complex and the transition state for reactions 1−3. These energy barriers are provided in Table 3. The energy barriers are 24.3, 19.43, and 10.38 kcal/mol for reactions 1−3, respectively. In both the intermediate-reactant complex and the transition state, the polar solvent effect plays a role in lowering the energy of the system. In the transition state, however, the stabilization of the ionic fragment pair makes a greater contribution to lowering the energy. Hence, each additional water molecule in reactions 1−3 lowers the energy of the transition state by a greater magnitude than the energy of the intermediate-reactant complex. Consequently, the energy barrier separating the intermediate-reactant complex and the transition state is decreased by the successive addition of water molecules in the reacting system.

TABLE 1: Relative Energies (kcal/mol) of Reactants, Reactant Complex, Transition State, Product Complex, and Products for Reactions 1−3 Calculated at the B3LYP/6-31+G(d) Level

	$n = 1$			$n = 2$			$n = 3$			$n = 4$		
species	E	ZPE	E'^{b}	E	ZPE	E'^{b}	E	ZPE	E'^{b}	E	ZPE	E'^{b}
$N_2O_5 + H_2O$	0^a	0^a	0^a	0^a	0^a	0^a	0^a	0^a	0^a	0^a	0^a	0^a
$N_2O_5(H_2O)_n$	−3.8	1.2	−2.6	−13.0	4.2	−8.9	−17.4	5.8	−11.6			
TS1	20.5	1.1	21.6	6.4	4.8	11.2	−7.0	7.0	0.			
$(HNO_3)_2(H_2O)_{n-1}$	−18.2	3.6	−14.5	−32.2	6.0	−26.2	−42.7	8.3	−34.3	−58.5		
$2HNO_3 + (n-1)H_2O$	−12.7	2.8	−9.9	−12.7	2.8	−9.9	−12.7	2.8	−9.9	−12.7	2.8	−9.9

[a] $E(N_2O_5) = -485.347\,651$ hartree, $ZPE(N_2O_5) = 16.79$ kcal/mol; $E(H_2O) = -76.422\,572$ hartree, ZPE = 13.24 kcal/mol. [b] $E' = E + ZPE$.

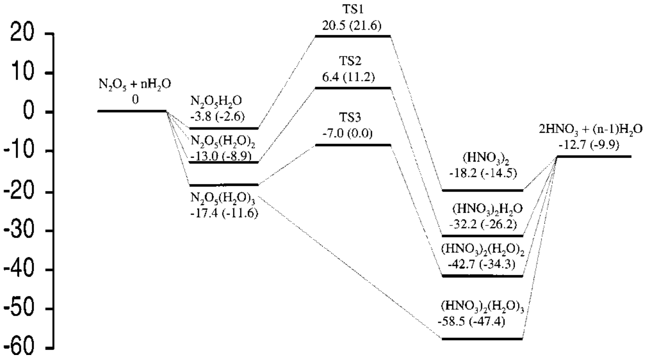

Figure 1. Energy level diagram for the stationary structures associated with reactions 1−4. Energies are in kcal/mol. Values in parentheses are zero-point corrected energies.

For reaction 4, we find that no intermediate-reactant complex can be identified and that the hydrolysis reaction proceeds directly from reactants to the product complex $(HNO_3)_2(H_2O)_3$ without an energy barrier. Therefore, the hydrolysis reaction involving four or more water molecules should involve no transition state and the reaction should proceed directly to products.

The activation energies reported above and in Figure 1 are based on kinetic mechanisms that are overall third order in reaction 2 and fourth order in reaction 3. In reality, the probability for the occurrence of a three-particle collision in reaction 2 is extremely low, and the probability for a four-particle collision is practically negligible. Any reliable analysis of the kinetics of the hydrolysis reaction requires that the appropriate relative energies be compared among the various reaction channels leading from reactants to the transition state. We are led, therefore, to consider all possible bimolecular reactions involved in the hydrolysis of N_2O_5 in which either two or three water molecules react overall. The relevant bimolecular reactions associated with the two- and three-water molecule hydrolysis of N_2O_5 are given in eqs 5 and 6 along with the relative energies (in kcal/mol, ZPE-corrected values are given in parentheses).

$$N_2O_5 + (H_2O)_2 \rightarrow TS2 \qquad E_a = 12.87\ (15.11) \quad (5a)$$

$$N_2O_5(H_2O) + H_2O \rightarrow TS2 \qquad E_a = 10.22\ (13.82) \quad (5b)$$

$$N_2O_5 + (H_2O)_3 \rightarrow TS3 \qquad E_a = 12.13\ (13.00) \quad (6a)$$

$$N_2O_5(H_2O) + (H_2O)_2 \rightarrow TS3 \qquad E_a = 3.19\ (6.57) \quad (6b)$$

$$N_2O_5(H_2O)_2 + H_2O \rightarrow TS3 \qquad E_a = 5.98\ (8.86) \quad (6c)$$

Comparison of the relative energies for the bimolecular reactions may provide information on the role of hydrogen bonding by H_2O in the N_2O_5 hydrolysis mechanism. The relative energies are smallest for the bimolecular reaction involving the monohydrated N_2O_5 cluster (reactions 5b and 6b). At low temperatures, therefore, we expect bimolecular reactions 5b and 6b to dominate with respect to two- and three-water reactions. The water molecule in the $N_2O_5{\cdot}H_2O$ complex may act as a hydrogen bond donor, making N_2O_5 more susceptible to a reacting water molecule. Reaction 1 is also bimolecular, it has a relatively large relative energy (about 20 kcal/mol). As a result, reaction 1 might be the only possible channel at very high temperatures where water clusters and $N_2O_5(H_2O)_n$ complexes are not present in significant amounts.

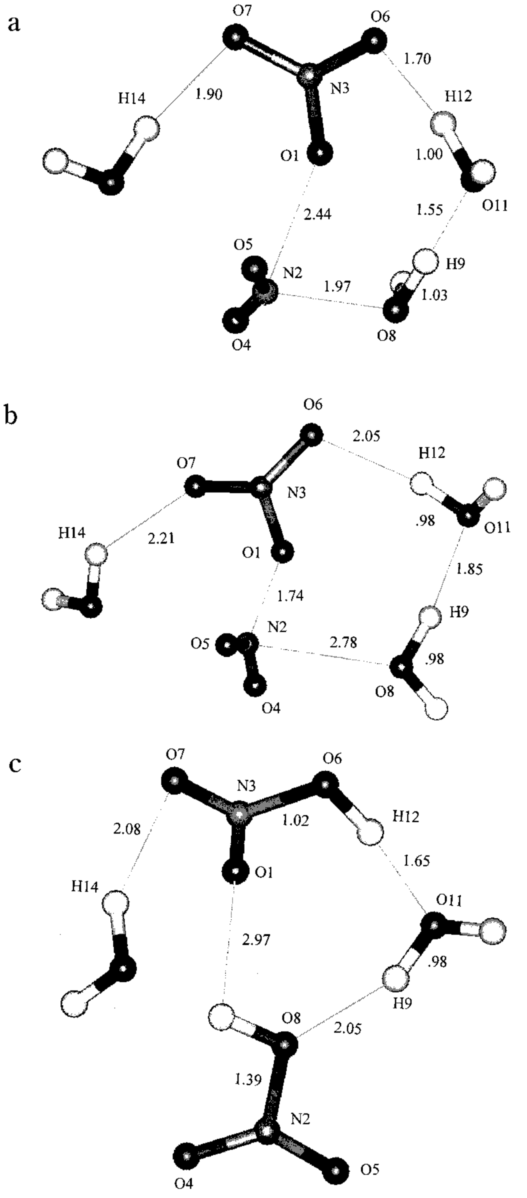

Figure 2. Optimized geometries for the pathway of reaction 3: $(HNO_3)_2(H_2O)_3 \rightarrow TS3 \rightarrow (HNO_3)_2(H_2O)_2$. Bond distances are in Å.

TABLE 2: Relative Energy (kcal/mol) and Selected Interatomic Distances (Å) on the Pathway of Reaction 3 from the Intrinsic Reaction Coordinate (IRC) Calculations

point[a]	energy	O1−N2	O8−N2	O8−H9	O11−H9	O11−H12	O6−H12
1	0.00	1.736	2.777	0.983	1.848	0.976	2.045
2	2.79	1.879	2.549	0.985	1.759	0.979	1.911
3	10.38	2.437	1.970	1.033	1.550	1.002	1.704
4	−0.97	3.465	1.505	1.583	1.039	1.329	1.165
5	−25.22	3.981	1.391	2.053	0.977	1.649	1.016

[a] Points 1, 3, and 5 are corresponding to the reactant complex, transition state, and product complex, respectively, whose structures are shown in Figure 2.

TABLE 3. Energy Barrier (kcal/mol) between the Intermediate-Reactant Complex and Transition State for Reactions 1−4

	$N_2O_5H_2O$	$N_2O_5(H_2O)_2$	$N_2O_5(H_2O)_3$	$N_2O_5(H_2O)_4$
barrier	24.3	19.43	10.38	<0
barrier + ZPE	24.2	20.1	17.42	<0

Since temperature decreases with altitude, the rates of reactions 5b and 6b might be expected to increase at higher altitudes. However, the water vapor partial pressure also decreases with increasing altitude. Hence, the actual dependency of the rates of reactions 5b and 6b on altitude will be determined by these two competing criteria. The two reaction channels should be favored at low temperatures, low altitudes, and high water vapor pressures.

Conclusions and Remarks

This study demonstrates that reactions 1−4 provide feasible pathways for the gas-phase homogeneous hydrolysis of N_2O_5 at various conditions. Increasing the number of water molecules in the reacting system progressively lowers the overall energy barrier for the reaction. The energy barrier between the intermediate-reactant complex and the transition state structure also decreases rapidly, and the presence of four water molecules completely eliminates the transition state. It therefore shows that the hydrolysis reaction will proceed at a rapid rate in water droplets, or regions in which high concentrations of water are present.

For the gas-phase hydrolysis of N_2O_5, reaction 1 is likely to be favored at high temperatures because of the large energy barrier and low probability for the existence of water clusters. At low temperatures, reactions 2 and 3 are expected to make a greater contribution due to the lower energy barriers and greater abundance of water clusters. However, on the basis of a comparison of the relative transition state energies for various bimolecular reactions between $N_2O_5(H_2O)_n$ and $(H_2O)_n$, it is found that reactions involving the monohydrated N_2O_5 complex should be accompanied by the largest rate constant for a given total number of water molecules.

The reduction of the reaction energy barrier for the hydrolysis of N_2O_5 with increasing numbers of water molecules may provide some insight into the heterogeneous mechanism, which is known experimentally to occur at a faster rate. The mechanism for reactions 2 and 3 involves a nucleophilic attack by a reacting water molecule. The extra water molecule provides additional stabilization, which lowers the activation energy for reactions 2 and 3. Surfaces that support heterogeneous catalysis contain active sites that can either directly absorb N_2O_5 to resemble the structure of the hydrated N_2O_5 complex or accept hydrogen bonds from water molecules to produce hydrated N_2O_5 complexes. Our results show that the N_2O_5 hydrolysis is kinetically favorable through hydrated N_2O_5 complexes, particularly the monohydrated complex. This might explain why surfaces promote hydrolysis of N_2O_5 at a faster rate than the gas-phase reaction with water molecules.

Acknowledgment. This work was supported in part by The Petroleum Research Fund (PRF Grant No. 30399-GB6), The Research Corp. (CC4121), The National Science Foundation (Research Experience for Undergraduates Program), The National Institute of Health (Minority Student Development Program), and The School of Science and Mathematics, California State University, Fullerton.

References and Notes

(1) Russell, A. G.; McRae, G. J.; Cass, G. R. *Atmos. Environ.* **1985**, *19*, 893.
(2) Koch, T. G.; Banham, S. F.; Sodeau, J. R.; Horn, A. B.; McCoustra, M. R. S.; Chesters, M. A. *J. Geophys. Res.* **1997**, *102*, 1513.
(3) Quinlan, M. A.; Reihs, C. M.; Golden, D. M.; Tolbert, M. A. *J. Phys. Chem.* **1990**, *94*, 3255.
(4) Hanson, D. R. *Geophys. Res. Lett.* **1997**, *24*, 1087.
(5) Wincel, H.; Mereand, E.; Castleman, A. W., Jr. *J. Phys. Chem.* **1994**, *98*, 8606.
(6) Mentel, T. H. F.; Bleilebens, D.; Wahner, A. *Atmos. Environ.* **1996**, *30*, 4007.
(7) Tauzon, E. C.; Atkinson, R.; Plum, C. N.; Winer, A. M.; Pitts, J. N., Jr. *Geophys Res. Lett.* **1983**, *10*, 953.
(8) Weschler, C. J.; Brauer, M.; Koutrakis, P. *Environ. Sci. Technol.* **1992**, *26*, 179.
(9) Morris E. D., Jr.; Niki, H. *J. Phys. Chem.* **1973**, *77*, 1929.
(10) Sverdrup, G. M.; Spicer, C. M.; Ward, G. F. *Int. J. Chem. Kinet.* **1987**, *19*, 191.
(11) Hanway, D.; Tao, F.-M, *Chem. Phys. Lett.* **1998**, *285*, 459.
(12) Becke, A. D. *J. Chem. Phys.* **1992**, *96*, 2155.
(13) Becke, A. D. *J. Chem. Phys.* **1992**, *97*, 9193.
(14) Becke, A. D. *J. Chem. Phys.* **1993**, *98*, 5648.
(15) Lee, C.; Yang, W.; Parr, R. G. *Phys. Rev. B* **1988**, *37*, 785.
(16) Peng, C.; Schlegel, H. B. *Isr. J. Chem.* **1993**, *33*, 449.
(17) Gonzalez, C.; Schlegel, H. B. *J. Chem. Phys.* **1989**, *90*, 2154.
(18) Frisch, M. J.; Trucks, G. W.; Schlegel, H. B.; Gill, P. M. W.; Johnson, B. G.; Robb, M. A.; Cheeseman, J. R.; Keith, T.; Petersson, G. A.; Montgomery, J. A.; Raghavachari, K.; Al-Laham, M. A.; Zakrzewski, V. G.; Ortiz, J. V.; Foresman, J. B.; Cioslowski, J.; Stefanov, B. B.; Nanayakkara, A.; Challacombe, M.; Peng, C. Y.; Ayala, P. Y.; Chen, W.; Wong, M. W.; Andres, J. L.; Replogle, E. S.; Gomperts, R.; Martin, R. L.; Fox, D. J.; Binkley, J. S.; Defrees, D. J.; Baker, J.; Stewart, J. P.; Head-Gordon, M.; Gonzalez, C.; Pople, J. A. *Gaussian 94*, Revision D.3; Gaussian, Inc.: Pittsburgh, PA, 1995.